

# Chiral coupled channel dynamics of the $\Lambda(1520)$ and the $K^-p \rightarrow \pi^0\pi^0\Lambda$ reaction

Sourav Sarkar, E. Oset and M.J. Vicente Vacas

Departamento de Física Teórica and IFIC, Centro Mixto Universidad de Valencia-CSIC,  
Institutos de Investigación de Paterna, Aptd. 22085, 46071 Valencia, Spain

May 23, 2019

## Abstract

We study the  $\Lambda(1520)$  in a chiral coupled channel approach. This resonance appears as dynamically generated from the interaction of the decuplet of baryons and the octet of mesons in  $s$ -wave with the inclusion of the  $\bar{K}N$  and  $\pi\Sigma$  channels in  $d$ -wave. Since the most important building block in the  $\Lambda(1520)$  is the  $\pi\Sigma^*(1385)$  channel, we study the  $K^-p \rightarrow \pi\Sigma^*(1385)(\pi^0\Lambda)$  reaction in the region of the  $\Lambda(1520)$  and above, and compare the results with recent experimental data. With the coupling of the  $\Lambda(1520)$  to the  $\pi\Sigma^*$  channel predicted by the theory we find a cross section in good agreement with the data and there is as well agreement for the invariant mass distributions which show a neat peak for the  $\Sigma^*(1385)$  in the  $(\pi^0\Lambda)$  spectrum. Predictions are made of a strong  $\Lambda(1520)$  resonant peak of the cross section, as a function of the  $K^-$  momentum, in the region below the measured data which, if confirmed experimentally, would give a stronger support to the idea of the  $\Lambda(1520)$  as a dynamically generated resonance.

# 1 Introduction

The unitary extensions of chiral perturbation theory,  $U\chi PT$ , are having a great impact in the study of meson baryon interaction at low energies and at the same time have shown that many known resonances listed by the Particle Data Group (PDG) [1] qualify as dynamically generated, or in simpler words, they are quasibound states of a meson and a baryon. After early studies in this direction showing that the  $\Lambda(1405)$  and the  $N^*(1535)$  were dynamically generated resonances [2, 3, 4, 5, 6, 7, 8, 9], more systematic studies have shown that there are two octets and one singlet of resonances from the interaction of the octet of pseudoscalar mesons with the octet of stable baryons [10, 11].

Further work in this direction [12, 13] has shown that many of the  $3/2^-$  low lying baryonic resonances appear as dynamically generated from the interaction of the decuplet of baryons and the octet of mesons. One of the interesting resonances generated in these schemes is the  $\Lambda(1520)$ . In this approach this resonance couples to the  $\pi\Sigma^*(1385)$  and  $K\Xi^*(1533)$  channels, particularly to the former one, to the point that being below the  $\pi\Sigma^*$  threshold, qualifies very well as a quasibound state of  $\pi\Sigma^*$ . However, the lack of other relevant channels which couple to the quantum numbers of the resonances makes the treatment of [12, 13] only semiquantitative. In particular, the  $\Lambda(1520)$  appears in [12, 13] at higher energy than the nominal one and with a relatively large width. This large width is a necessary consequence of the large coupling to the  $\pi\Sigma^*$  channel and the fact that the pole appears at energies above the  $\pi\Sigma^*$  threshold. On the other hand, if we modify the subtraction constants of the meson baryon loop function to bring the pole below the  $\pi\Sigma^*$  threshold, then the pole appears without imaginary part. Since the width of the  $\Lambda(1520)$  resonance comes basically from the decay into the  $\bar{K}N$  and  $\pi\Sigma(1193)$ , the introduction of these channels is mandatory to reproduce the shape of the  $\Lambda(1520)$  resonance.

In the present work we include the  $\bar{K}N$  and  $\pi\Sigma$  channels into the set of coupled channels which build up the  $\Lambda(1520)$ . The novelty with respect to the other channels already accounted for [12, 13], which couple in  $s$ -wave, is that the new channels couple in  $d$ -waves. Fitting two parameters to the partial decay widths of the  $\Lambda(1520)$  into  $\bar{K}N$  and  $\pi\Sigma$ , a good shape for the  $\Lambda(1520)$  dominated amplitudes is obtained at the right position and with the proper experimental width. The coupling of the  $\Lambda(1520)$  to the  $\pi\Sigma^*$  channel is a prediction of the theory and we use this to study the reaction  $K^-p \rightarrow \pi\Sigma(1385)(\pi^0\Lambda)$  which is closely related to the strength of this coupling. We then compare with recent experimental results measured above the  $\Lambda(1520)$  energy. The agreement with the data is good and the cross section is sizeable thanks to the large coupling of the  $\Lambda(1520)$  to the  $\pi\Sigma^*$  channel. Other standard mechanisms for the  $K^-p \rightarrow \pi^0\pi^0\Lambda$  reaction without the  $\Lambda(1520)$  give too small a cross section compared to experiment in a wide range of energies around the  $\Lambda(1520)$  peak.

We also compare the invariant mass distributions for  $\pi^0\Lambda$ , where a distinct peak associated to the  $\Sigma(1385)$  resonance is seen, in good agreement with experiment.

We also make predictions for the cross section for  $K^-p$  energies around the  $\Lambda(1520)$ , where we find a large peak with the  $\Lambda(1520)$  shape, not measured so far, and which, if confirmed experimentally, would give a strong support to the idea of the  $\Lambda(1520)$  as a

dynamically generated resonance.

Inclusion of the new channels  $\bar{K}N$  and  $\pi\Sigma$  into the coupled channel approach allows one to calculate the cross sections of other reactions where the  $\Lambda(1520)$  appears, much as has been the case of the  $\Lambda(1405)$  [14], where a large variety of reactions could be studied within the chiral unitary approach taking into account that the  $\Lambda(1405)$  is dynamically generated from the  $\bar{K}N$  and coupled channels in  $s$ -wave.

## 2 Decuplet octet interaction and the $\Lambda(1520)$

Following [13], we briefly recall how the  $\Lambda(1520)$  is generated dynamically in the  $s$ -wave interaction of the decuplet of baryons with the octet of pseudoscalar mesons. We consider the lowest order term of the chiral Lagrangian given by [15]

$$\mathcal{L} = -i\bar{T}^\mu \not{\mathcal{D}} T_\mu \quad (1)$$

where  $T_{abc}^\mu$  is the spin decuplet field and  $\mathcal{D}^\nu$  the covariant derivative given by

$$\mathcal{D}^\nu T_{abc}^\mu = \partial^\nu T_{abc}^\mu + (\Gamma^\nu)_a^d T_{dbc}^\mu + (\Gamma^\nu)_b^d T_{adc}^\mu + (\Gamma^\nu)_c^d T_{abd}^\mu \quad (2)$$

with  $\mu$  the Lorentz index and  $a, b, c$  the  $SU(3)$  indices. The vector current  $\Gamma^\nu$  is given by

$$\Gamma^\nu = \frac{1}{2}(\xi \partial^\nu \xi^\dagger + \xi^\dagger \partial^\nu \xi) \quad (3)$$

with

$$\xi^2 = U = e^{i\sqrt{2}\Phi/f} \quad (4)$$

where  $\Phi$  is the  $3 \times 3$  matrix of fields for the pseudoscalar mesons [16] and  $f = 93$  MeV. Consideration of only the  $s$ -wave part of the baryon meson interaction and the use of non-relativistic approximations as described in detail in [13] allows for substantial technical simplifications.

We obtain the  $s$ -wave transition amplitudes for a meson of incoming and outgoing momentum  $k$  and  $k'$  respectively as

$$V_{ij} = -\frac{1}{4f^2} C_{ij} (k^0 + k'^0). \quad (5)$$

For the quantum numbers  $S = -1$  and  $I = 0$  the relevant channels are  $\pi\Sigma^*$  and  $K\Xi^*$ . The corresponding coefficients  $C_{ij}$  are shown in table 1 where we have used the isospin states<sup>1</sup>

$$\begin{aligned} |\pi\Sigma^*; I = 0\rangle &= \frac{1}{\sqrt{3}} |\pi^-\Sigma^{*+}\rangle - \frac{1}{\sqrt{3}} |\pi^0\Sigma^{*0}\rangle - \frac{1}{\sqrt{3}} |\pi^+\Sigma^{*-}\rangle \\ |K\Xi^*; I = 0\rangle &= -\frac{1}{\sqrt{2}} |K^0\Xi^{*0}\rangle + \frac{1}{\sqrt{2}} |K^+\Xi^{*-}\rangle. \end{aligned} \quad (6)$$

---

<sup>1</sup>we use  $|\pi^+\rangle = -|1\ 1\rangle$

	$\pi\Sigma^*$	$K\Xi^*$
$\pi\Sigma^*$	4	$-\sqrt{6}$
$K\Xi^*$	$-\sqrt{6}$	3

Table 1:  $C_{ij}$  coefficients for  $S = -1$ ,  $I = 0$ .

The matrix  $V$  is then used as the kernel of the Bethe-Salpeter equation to obtain the unitary transition matrix [4]. This results in the matrix equation

$$T = (1 - VG)^{-1}V \quad (7)$$

where  $G$  is a diagonal matrix representing the meson-baryon loop function

$$G_l = i \int \frac{d^4q}{(2\pi)^4} \frac{M_l}{E_l(\vec{q})} \frac{1}{\sqrt{s} - q^0 - E_l(\vec{q}) + i\epsilon} \frac{1}{q^2 - m_l^2 + i\epsilon} \quad (8)$$

in which  $M_l$  and  $m_l$  are the masses of the baryons and mesons respectively. In the dimensional regularization scheme this is given by

$$\begin{aligned} G_l &= i 2M_l \int \frac{d^4q}{(2\pi)^4} \frac{1}{(P - q)^2 - M_l^2 + i\epsilon} \frac{1}{q^2 - m_l^2 + i\epsilon} \\ &= \frac{2M_l}{16\pi^2} \left\{ a_l(\mu) + \ln \frac{M_l^2}{\mu^2} + \frac{m_l^2 - M_l^2 + s}{2s} \ln \frac{m_l^2}{M_l^2} - 2i\pi \frac{q_l}{\sqrt{s}} \right. \\ &\quad \left. + \frac{q_l}{\sqrt{s}} [\ln(s - (M_l^2 - m_l^2) + 2q_l\sqrt{s}) + \ln(s + (M_l^2 - m_l^2) + 2q_l\sqrt{s}) \right. \\ &\quad \left. - \ln(s - (M_l^2 - m_l^2) - 2q_l\sqrt{s}) - \ln(s + (M_l^2 - m_l^2) - 2q_l\sqrt{s})] \right\}, \quad (9) \end{aligned}$$

where  $\mu$  is the scale of dimensional regularization,  $a_l$  is the subtraction constant and  $q_l$  denotes the three-momentum of the meson or baryon in the centre of mass frame. We then look for poles of the transition matrix  $T$  in the complex  $\sqrt{s}$  plane. The complex poles,  $z_R$ , appear in unphysical Riemann sheets. In the present work we use the loop function of eq. (9) for energies below threshold and replace it above threshold with

$$G_l^{2nd} = G_l + 2i \frac{q_l}{\sqrt{s}} \frac{M_l}{4\pi} \quad (10)$$

where the variables on the right hand side of the above equation are evaluated in the first (physical) Riemann sheet. It is trivially verified that the same can be achieved by changing the sign of the complex valued momentum  $q_l$  from positive to negative in the loop function  $G_l(z)$  of eq. (9) for the channels which are above threshold at an energy equal to  $\text{Re}(z)$ . This we call the second Riemann sheet  $R_2$ .

Using the natural size values [6]  $a = -2$  and  $\mu = 700$  MeV, we find a pole at  $z_R = 1550 - i67$  as seen in fig. 1, which we can well associate with the 4-star resonance  $\Lambda(1520)$ .

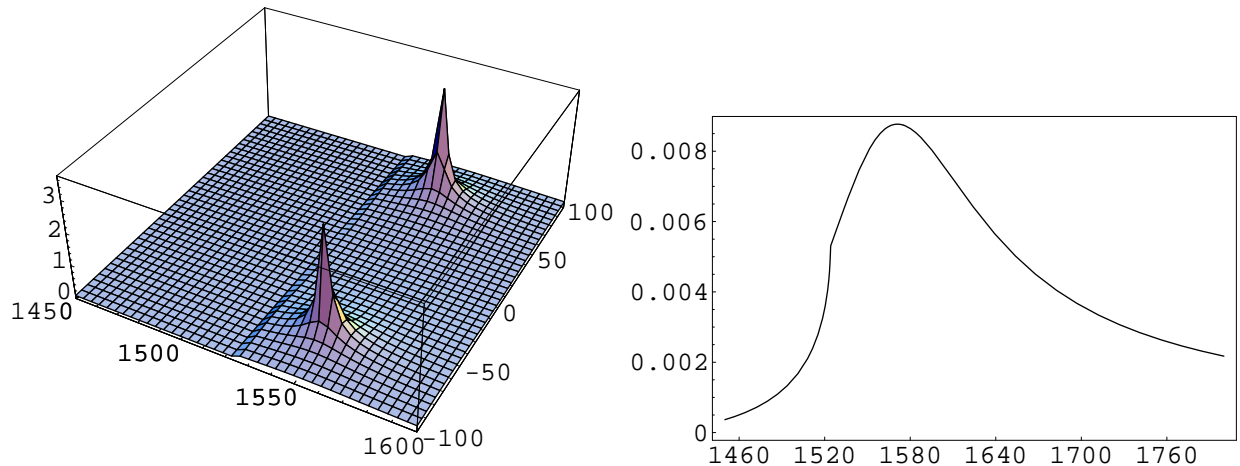


Figure 1: Left: The  $\Lambda(1520)$  pole as seen in the  $\pi\Sigma^* \rightarrow \pi\Sigma^*$  amplitude in the complex  $\sqrt{s}$  plane. Right:  $|T_{\pi\Sigma^* \rightarrow \pi\Sigma^*}|^2$  in  $(\text{MeV}^{-2})$ .

The residue at this pole indicates a strong coupling to the  $\pi\Sigma^*$  channel [13]. However, the experimental mass and width are lower and there are also large branching ratios of the  $\Lambda(1520)$  to the  $\bar{K}N$  and  $\pi\Sigma$  channels. In the following section we will phenomenologically add these channels to our coupled channel scheme.

### 3 Introduction of the $\bar{K}N$ and $\pi\Sigma$ channels

We will generate the resonance  $\Lambda(1520)$  in coupled channels involving the  $\pi\Sigma^*$ ,  $K\Xi^*$ ,  $\bar{K}N$  and  $\pi\Sigma$ . However, we shall only couple the  $\bar{K}N$  and  $\pi\Sigma$  channels to the dominant  $\pi\Sigma^*$  channel as described below.

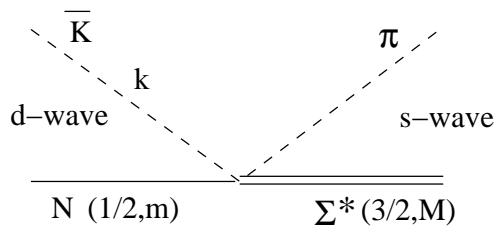


Figure 2: The  $\bar{K}N \rightarrow \pi\Sigma^*$  vertex

Consider the transition  $\bar{K}N$  ( $d$ -wave) to  $\pi\Sigma^*$  ( $s$ -wave) as shown in fig. 2. We start with an amplitude of the form

$$-it_{\bar{K}N \rightarrow \pi\Sigma^*} = -i\beta_{\bar{K}N} |\vec{k}|^2 \left[ T^{(2)\dagger} \otimes Y_2(\hat{k}) \right]_{00} \quad (11)$$

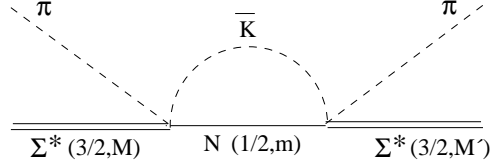


Figure 3:  $\pi\Sigma^* \rightarrow \pi\Sigma^*$  through  $\bar{K}N$  loop arising in the Bethe-Salpeter series

where  $T^{(2)\dagger}$  is a (rank 2) spin transition operator defined by

$$\langle 3/2 \ M | T^{(2)\dagger} | 1/2 \ m \rangle = \mathcal{C}(1/2 \ 2 \ 3/2; m \ \mu \ M) \langle 3/2 || T^{(2)\dagger} || 1/2 \rangle ,$$

$Y_2(\hat{k})$  is the spherical harmonic coupled to  $T^{(2)\dagger}$  to produce a scalar, and  $\vec{k}$  is the momentum of the  $\bar{K}$ . The 3rd component of spin of the initial nucleon and the final  $\Sigma^*$  are denoted by  $m$  and  $M$  respectively. Choosing appropriately the reduced matrix element we obtain

$$-it_{\bar{K}N \rightarrow \pi\Sigma^*} = -i\beta_{\bar{K}N} |\vec{k}|^2 \mathcal{C}(1/2 \ 2 \ 3/2; m, M - m) Y_{2, m-M}(\hat{k}) (-1)^{M-m} \sqrt{4\pi}. \quad (12)$$

In the same way we write the amplitude for  $\pi\Sigma$  ( $d$ -wave) to  $\pi\Sigma^*$  ( $s$ -wave) as

$$-it_{\pi\Sigma \rightarrow \pi\Sigma^*} = -i\beta_{\pi\Sigma} |\vec{k}|^2 \mathcal{C}(1/2 \ 2 \ 3/2; m, M - m) Y_{2, m-M}(\hat{k}) (-1)^{M-m} \sqrt{4\pi}. \quad (13)$$

Now, let us consider fig. 3. The loop function  $G$  involving the  $\bar{K}$  and  $N$  is given by

$$\begin{aligned} G &= i \int \frac{d^4q}{(2\pi)^4} G_N D_{\bar{K}} 4\pi \\ &\quad \beta_{\bar{K}N} |\vec{q}|^2 \sum_m \mathcal{C}(1/2 \ 2 \ 3/2; m, M' - m) Y_{2, m-M'}(\hat{q}) (-1)^{M'-m} \\ &\quad \beta_{\bar{K}N} |\vec{q}|^2 \mathcal{C}(1/2 \ 2 \ 3/2; m, M - m) Y_{2, m-M}^*(\hat{q}) (-1)^{M-m} \end{aligned} \quad (14)$$

where  $G_N$  and  $D_{\bar{K}}$  are the propagators for the nucleon and the  $\bar{K}$  respectively. Eq. (14) can be further simplified by performing the angular integration of the two spherical harmonics, which gives  $\delta_{MM'}$  and then using the orthogonality of the Clebsch Gordan (CG) coefficients. We obtain

$$\begin{aligned} G &= i \delta_{MM'} \int \frac{dq^0}{2\pi} \int \frac{|\vec{q}|^2 d|\vec{q}|}{(2\pi)^3} 4\pi (\beta_{\bar{K}N} |\vec{q}|^2)^2 \\ &\quad \frac{1}{q^2 - m_K^2 + i\epsilon} \frac{M_N}{E_N(\vec{q})} \frac{1}{\sqrt{s} - q^0 - E_N(\vec{q}) + i\epsilon} \\ &= i \delta_{MM'} \int \frac{d^4q}{(2\pi)^4} (\beta_{\bar{K}N} |\vec{q}|^2)^2 \frac{M_N}{E_N(\vec{q})} \frac{1}{q^2 - m_K^2 + i\epsilon} \frac{1}{\sqrt{s} - q^0 - E_N(\vec{q}) + i\epsilon}. \end{aligned} \quad (15)$$

Factorizing the vertex, i.e.  $|\vec{q}|^2$ , on shell as done in the Bethe Salpeter approach [4] which is justified by the underlying N/D unitarization method [18, 6] results in the simplification that we can use the transition matrix elements

$$\begin{aligned} V_{\bar{K}N \rightarrow \pi\Sigma^*} &= \beta_{\bar{K}N} |\vec{q}_{on}|^2 \\ V_{\pi\Sigma \rightarrow \pi\Sigma^*} &= \beta_{\pi\Sigma} |\vec{q}'_{on}|^2 \end{aligned} \quad (16)$$

where  $\vec{q}_{on}$  and  $\vec{q}'_{on}$  are the (on-shell) CM momenta of the  $\bar{K}$  and  $\pi$  respectively for a given value of  $s$ . After removing the factor  $(\beta_{\bar{K}N}|\vec{q}|^2)^2$  in eq. (15), the rest of the formula is the ordinary  $G$  function for the  $s$ -wave meson baryon interaction, eq. (8). This allows us to use the same formalism as in ordinary  $s$ -wave scattering assuming an effective transition potential  $\beta_{\bar{K}N}|q_{on}|^2$  for  $\pi\Sigma^* \rightarrow \bar{K}N$ .

With the matrix  $V$  now given by

$$V = \begin{vmatrix} V_{\pi\Sigma^* \rightarrow \pi\Sigma^*} & V_{\pi\Sigma^* \rightarrow K\Xi^*} & \beta_{\bar{K}N}|\vec{q}_{on}|^2 & \beta_{\pi\Sigma}|\vec{q}'_{on}|^2 \\ V_{K\Xi^* \rightarrow \pi\Sigma^*} & V_{K\Xi^* \rightarrow K\Xi^*} & 0 & 0 \\ \beta_{\bar{K}N}|\vec{q}_{on}|^2 & 0 & 0 & 0 \\ \beta_{\pi\Sigma}|\vec{q}'_{on}|^2 & 0 & 0 & 0 \end{vmatrix}, \quad (17)$$

we solve eq. (7) to obtain the amplitudes  $T$ . The actual transition amplitudes are related to  $T$  through the following relations

$$\begin{aligned} t_{\pi\Sigma^* \rightarrow \pi\Sigma^*} &= T_{\pi\Sigma^* \rightarrow \pi\Sigma^*} \\ t_{\bar{K}N \rightarrow \pi\Sigma^*} &= T_{\bar{K}N \rightarrow \pi\Sigma^*} \mathcal{C}(1/2 \ 2 \ 3/2; m, M-m) Y_{2,m-M}(\hat{k}) (-1)^{M-m} \sqrt{4\pi} \\ t_{\pi\Sigma \rightarrow \pi\Sigma^*} &= T_{\pi\Sigma \rightarrow \pi\Sigma^*} \mathcal{C}(1/2 \ 2 \ 3/2; m, M-m) Y_{2,m-M}(\hat{k}) (-1)^{M-m} \sqrt{4\pi} \\ t_{\bar{K}N \rightarrow \bar{K}N} &= T_{\bar{K}N \rightarrow \bar{K}N} \sum_M \mathcal{C}(1/2 \ 2 \ 3/2; m, M-m) Y_{2,m-M}(\hat{k}) \\ &\quad \mathcal{C}(1/2 \ 2 \ 3/2; m', M-m') Y_{2,m'-M}(\hat{k}) (-1)^{m'-m} 4\pi. \end{aligned} \quad (18)$$

We then look for poles in the 2nd Riemann sheet of the complex plane. Assuming that the pole corresponding to the  $\Lambda(1520)$  appears at  $z = z_R$  where  $z$  stands for the (complex) CM energy, the amplitudes close to the pole can be written as

$$\begin{aligned} T_{\pi\Sigma^* \rightarrow \pi\Sigma^*} &= \frac{g_{\pi\Sigma^*}^2}{z - z_R} \\ T_{\bar{K}N \rightarrow \pi\Sigma^*} &= \frac{g_{\pi\Sigma^*} g_{\bar{K}N}}{z - z_R} \\ T_{\pi\Sigma \rightarrow \pi\Sigma^*} &= \frac{g_{\pi\Sigma^*} g_{\pi\Sigma}}{z - z_R} \end{aligned} \quad (19)$$

where the couplings  $g_{\pi\Sigma^*}$ ,  $g_{\bar{K}N}$  and  $g_{\pi\Sigma}$  can be obtained from the residues at the pole.

Writing the amplitudes for the  $\Lambda(1520)$  decay to  $\bar{K}N$  and  $\pi\Sigma$  respectively as,

$$\begin{aligned} -it_{\Lambda(1520) \rightarrow \bar{K}N} &= -ig_{\bar{K}N} \mathcal{C}(1/2 \ 2 \ 3/2; m, M-m) Y_{2,m-M}^*(\hat{k}) (-1)^{M-m} \sqrt{4\pi} \\ -it_{\Lambda(1520) \rightarrow \pi\Sigma} &= -ig_{\pi\Sigma} \mathcal{C}(1/2 \ 2 \ 3/2; m, M-m) Y_{2,m-M}^*(\hat{k}) (-1)^{M-m} \sqrt{4\pi} \end{aligned} \quad (20)$$

the partial decay widths of the  $\Lambda(1520)$  are obtained as,

$$\begin{aligned} \Gamma_{\bar{K}N} &= \frac{g_{\bar{K}N}^2}{2\pi} \frac{M_N}{M_\Lambda} k_{\bar{K}} \\ \Gamma_{\pi\Sigma} &= \frac{g_{\pi\Sigma}^2}{2\pi} \frac{M_\Sigma}{M_\Lambda} k_\pi \end{aligned} \quad (21)$$

where  $k_{\bar{K}} = |\vec{q}_{on}| = 242$  MeV and  $k_{\pi} = |\vec{q}'_{on}| = 263$  MeV. The partial decay width to the  $\pi\Sigma^*$  channel is zero because the  $\Lambda(1520)$  pole is below the threshold for this channel. Note that  $g_{\bar{K}N}$  and  $g_{\pi\Sigma}$  automatically incorporate the  $\beta_{\bar{K}N}|\vec{q}_{on}|^2$  and  $\beta_{\pi\Sigma}|\vec{q}'_{on}|^2$  of the transition potential since at least one  $\pi\Sigma^* \rightarrow \bar{K}N$  transition is needed in the Bethe Salpeter series. Hence the term  $|\vec{q}_{on}|^4 k_{\bar{K}} = k_{\bar{K}}^5$  guarantees the  $d$ -wave character of the decay.

We vary  $\beta_{\bar{K}N}$  and  $\beta_{\pi\Sigma}$  to reproduce the correct partial decay widths of the  $\Lambda(1520)$  into  $\bar{K}N(45\%)$  and  $\pi\Sigma(42\%)$  out of a total width of 15.6 MeV and simultaneously the subtraction constant  $a$  in order to have the pole at the experimental  $\Lambda(1520)$  mass. This exercise results in the values  $|g_{\pi\Sigma^*}| = 1.57$ ,  $|g_{\bar{K}N}| = 0.54$  and  $|g_{\pi\Sigma}| = 0.45$  for the couplings of the various channels to  $\Lambda(1520)$  using  $\beta_{\bar{K}N} = 2.4 \times 10^{-7}$ ,  $\beta_{\pi\Sigma} = 1.7 \times 10^{-7}$  in units of  $\text{MeV}^{-3}$  and  $a = -2.5$ , fixing  $\mu = 700$  MeV. With this we obtain the  $\Lambda(1520)$  pole at the position  $z_R = 1519.7 - i7.9$  as seen in fig. 4.

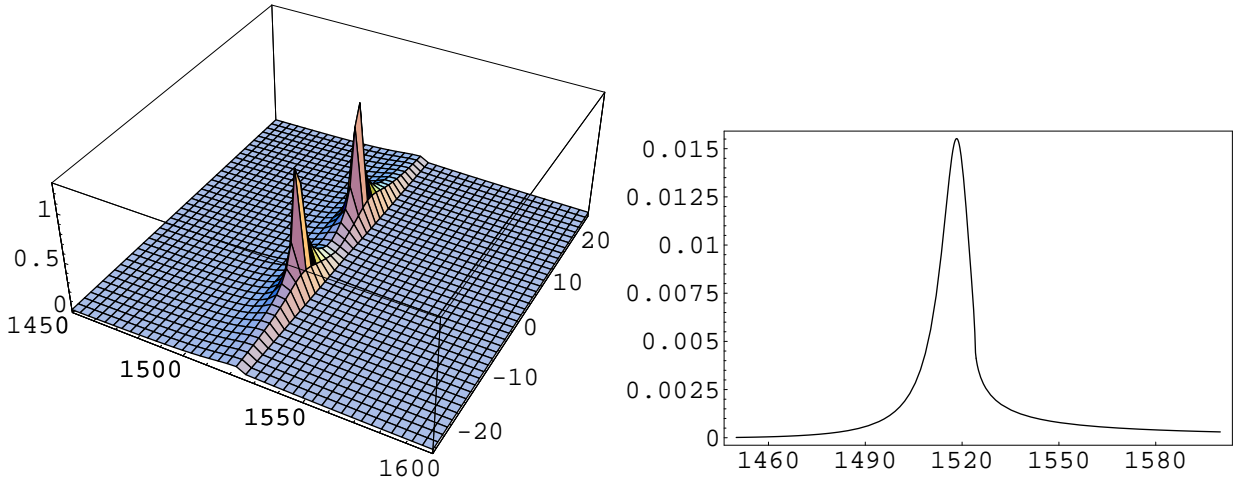


Figure 4: Left: The  $\Lambda(1520)$  pole as seen in the  $\bar{K}N \rightarrow \pi\Sigma^*$  amplitude in the complex  $\sqrt{s}$  plane. Right:  $|T_{\bar{K}N \rightarrow \pi\Sigma^*}|^2$  in  $(\text{MeV}^{-2})$ .

The isoscalar part of the amplitudes for specific charge channels can be obtained from the amplitudes obtained above, using<sup>2</sup>

$$\begin{aligned}
|\pi\Sigma; I=0\rangle &= -\frac{1}{\sqrt{3}} |\pi^-\Sigma^+\rangle - \frac{1}{\sqrt{3}} |\pi^0\Sigma^0\rangle - \frac{1}{\sqrt{3}} |\pi^+\Sigma^-\rangle \\
|\bar{K}N; I=0\rangle &= \frac{1}{\sqrt{2}} |\bar{K}^0n\rangle + \frac{1}{\sqrt{2}} |K^-p\rangle
\end{aligned} \tag{22}$$

and multiplying the  $I=0$  amplitudes obtained above by the relevant CG coefficients. It is to be noted that  $\beta_{\bar{K}N}$  and  $\beta_{\pi\Sigma}$  have been fitted to the partial decay widths. Hence we are not making any prediction for these couplings, or equivalently  $g_{\bar{K}N}$  and  $g_{\pi\Sigma}$ . However, the coupling  $g_{\pi\Sigma^*}$  is a prediction of the theory, up to small changes in the fine tuning of the subtraction constant.

<sup>2</sup>we use  $|K^-\rangle = -|\frac{1}{2} \frac{1}{2}\rangle$  and  $|\Sigma^+\rangle = -|11\rangle$

## 4 The reaction $K^-p \rightarrow \pi^0 \Sigma^{*0}(1385) \rightarrow \pi^0 \pi^0 \Lambda(1116)$

Here we evaluate the cross-section for the reaction  $K^-p \rightarrow \pi^0 \Sigma^{*0}$  generated by the coupled channel scheme and the subsequent decay of the  $\Sigma^{*0}(1385)$  to  $\pi^0 \Lambda(1116)$  as shown in fig. 5.

To obtain the cross-section for  $K^-p \rightarrow \pi^0 \Sigma^{*0}$  in the  $K^-p$  CM frame we use the formula

$$\frac{d\sigma}{d\Omega} = \frac{1}{16\pi^2} \frac{M_N M_{\Sigma^*}}{s} \frac{|\vec{p}_1|}{k} \sum_i \sum_f |t_{K^-p \rightarrow \pi^0 \Sigma^{*0}}|^2 \quad (23)$$

where  $|\vec{p}_1|$  and  $\vec{k} = (0, 0, k)$  denote the momenta of the outgoing pion and the incoming kaon respectively. Using eq. (18) and  $Y_{2,m-M}(\hat{k}) = \sqrt{\frac{5}{4\pi}} \delta_{mM}$  and taking into account the CG coefficients we find

$$t_{K^-p \rightarrow \pi^0 \Sigma^{*0}} = \sqrt{\frac{1}{3}} T_{\bar{K}N \rightarrow \pi \Sigma^*} \delta_{mM} \begin{Bmatrix} -1 & m = +1/2 \\ +1 & m = -1/2 \end{Bmatrix} \quad (24)$$

where  $m$  is the spin of the proton and  $M$  that of the  $\Sigma^{*0}$ . The cross section is then given by

$$\sigma = \frac{1}{12\pi} \frac{M_N M_{\Sigma^*}}{s} \frac{|\vec{p}_1|}{k} |T_{\bar{K}N \rightarrow \pi \Sigma^*}|^2. \quad (25)$$

To obtain the cross section for  $K^-p \rightarrow \pi^0 \Sigma^{*0} \rightarrow \pi^0 \pi^0 \Lambda$  we now evaluate the Feynman diagram of fig. 5 where the  $\Sigma^{*0}$  appears as a particle propagator.

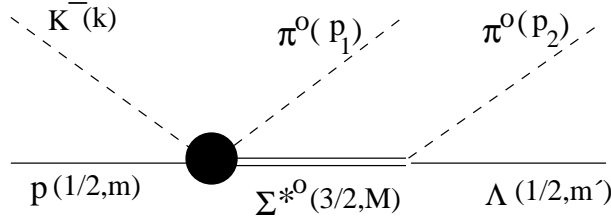


Figure 5: Scheme for  $K^-p \rightarrow \pi^0 \Sigma^{*0}(1385) \rightarrow \pi^0 \pi^0 \Lambda(1116)$ . The blob indicates the unitarized vertex.

The vertex  $\Sigma^{*0} \rightarrow \pi^0 \Lambda$  is given by [19]

$$-it_{\pi^0 \Lambda \rightarrow \Sigma^{*0}} = -\frac{f_{\Sigma^* \pi \Lambda}}{m_\pi} \vec{S}^\dagger \cdot \vec{p}'_2 \quad (26)$$

where  $S^\dagger$  is the 1/2 to 3/2 spin transition operator and the coupling  $f_{\Sigma^* \pi \Lambda}$  is fitted to the partial decay width of 32 MeV for  $\Sigma^{*0} \rightarrow \pi^0 \Lambda$ . Using the  $SU(3)$  arguments of [19] one obtains  $\frac{f_{\Sigma^* \pi \Lambda}}{m_\pi} = \frac{6}{5} \frac{D+F}{2f}$ . The amplitude for the process shown in fig. 5 in the  $K^-p$  CM is then obtained as

$$-it(\vec{p}_1, \vec{p}_2) = \frac{-iT_{\bar{K}N \rightarrow \pi \Sigma^*}}{3\sqrt{2}} \frac{f_{\Sigma^* \pi \Lambda}/m_\pi}{M_R - M_{\Sigma^*} + i\Gamma_{\Sigma^*}(M_R)/2} \begin{Bmatrix} -2p'_{2z} & m' = +1/2 \\ p'_{2x} + ip'_{2y} & m' = -1/2 \end{Bmatrix} \quad (27)$$

where  $m'$  is the spin of the outgoing  $\Lambda$ . Here, and in the following we will take the spin projection  $m = +1/2$  for the proton. The  $p$ -wave decay width of the propagating  $\Sigma^*$  is given by

$$\Gamma_{\Sigma^*}(M_R) = \frac{1}{6\pi} \frac{f_{\Sigma^*\pi\Lambda}^2}{m_\pi^2} \frac{M_\Lambda}{M_R} |\vec{p}'_2|^3 \quad (28)$$

from where we obtain  $f_{\Sigma^*\pi\Lambda} = 1.3$  for  $M_R = M_{\Sigma^*}$ , which only differs from the  $SU(3)$  value given above by about 10%. The momentum  $\vec{p}'_2$  of the final pion in the rest system of the  $\Sigma^*$  is obtained as

$$\vec{p}'_2 = \left[ \left( \frac{E_R}{M_R} - 1 \right) \frac{(\vec{p}_2 \cdot \vec{p}_1)}{|\vec{p}_1|^2} + \frac{p_2^0}{M_R} \right] \vec{p}_1 + \vec{p}_2 \quad (29)$$

where  $M_R^2 = (p_2 + p_\Lambda)^2$  and  $E_R^2 = \vec{p}_1^2 + M_R^2$ .

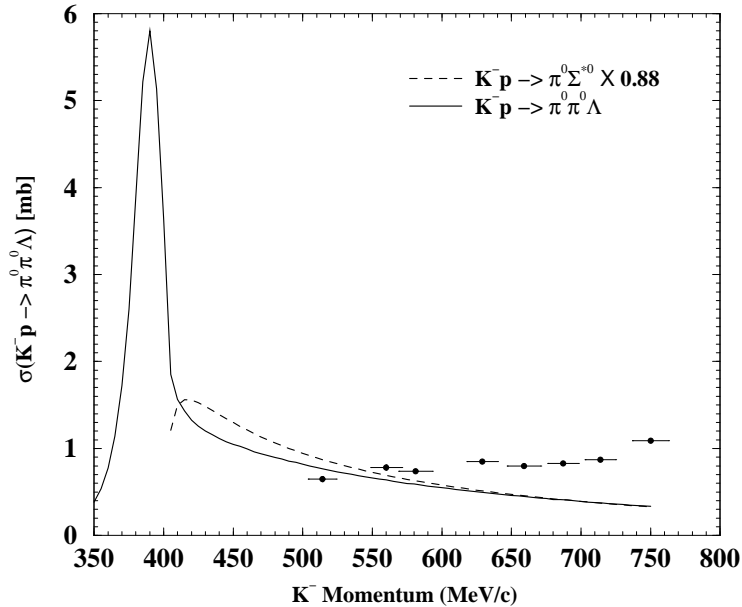


Figure 6: Cross-section as a function of the  $K^-$  momentum

In the next step, the total squared amplitude for  $K^-p \rightarrow \pi^0\pi^0\Lambda$  is symmetrized in the momenta  $\vec{p}_1$  and  $\vec{p}_2$  to account for the two  $\pi^0$ s in the final state so that,

$$|Amp|^2 = \sum_{m'} |t(\vec{p}_1, \vec{p}_2) + t(\vec{p}_2, \vec{p}_1)|^2. \quad (30)$$

The cross section is then obtained by integrating the above amplitude over the three-particle phase space (with a factor 1/2 for the identity of the two pions). Details are discussed in the appendix. The results are shown in fig. 6. The peak in the cross section for  $K^-p \rightarrow \pi^0\pi^0\Lambda$  (solid line) corresponds to the  $\Lambda(1520)$ . We observe a fair agreement with the experimental data [20] in the region of  $K^-$  momenta up to about 600 MeV from where other mechanisms for  $\pi^0\pi^0\Lambda$  not tied to  $\pi^0\Sigma^{*0}$  production become more relevant as

we shall see. The cross section for  $K^-p \rightarrow \pi^0\Sigma^{*0}$  multiplied by the  $\Sigma^* \rightarrow \Lambda\pi$  branching ratio (=0.88) is also shown for comparison (dashed line). Recall that the threshold for this reaction lies just above the peak of the  $\Lambda(1520)$ . It is interesting to see that there is a good agreement between the two methods of calculation when we are above the  $\pi^0\Sigma^{*0}$  threshold. However, evaluating the  $K^-p \rightarrow \pi^0\Sigma^{*0}$  cross section, assuming the  $\Sigma^{*0}$  as a stable particle gives no cross section below the  $\pi^0\Sigma^{*0}$  threshold and then the explicit evaluation of  $K^-p \rightarrow \pi^0\pi^0\Lambda$  using the  $\Sigma^{*0}$  propagator becomes mandatory and provides strength below this threshold. This feature is rather interesting because one can see the shape of the  $\Lambda(1520)$  in the cross section as a function of the  $K^-$  momentum. The strength of this peak is a genuine prediction of the theory, as well as the strength predicted around 500–600 MeV/c  $K^-$  momentum.

It would be instructive to get data around the energy of the peak, since it would be a clean proof of the link between the  $\Lambda(1520)$  and the  $\pi\Sigma^*$  channel which is the basic prediction of the chiral unitary approach.

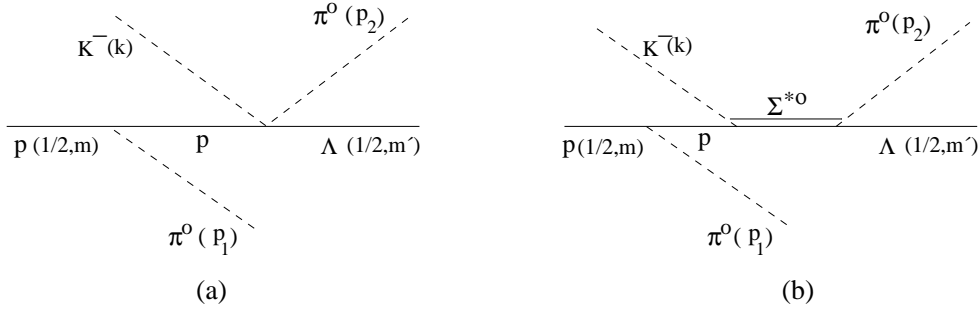


Figure 7: A conventional scheme for  $K^-p \rightarrow \pi^0\pi^0\Lambda$

We will now consider other mechanisms, figs. 7 and 8 which are not tied to the  $\Lambda(1520)$  resonance. In fig. 7 we separate the  $K^-p \rightarrow \pi^0\Lambda$  interaction in  $s$ -wave (a) and  $p$ -wave (b), this latter one dominated by the  $\Sigma^*$  pole [21]. Since there is no  $s$ -wave resonance in  $\pi^0\Lambda$  around the energies we investigate, it is enough to take for  $K^-p \rightarrow \pi^0\Lambda$  the lowest order chiral amplitude in  $s$ -wave in fig. 7(a), which we get from [4], and we obtain for the amplitude of this diagram,

$$-it^{(s\text{-wave})} = \frac{\sqrt{3}}{2} \frac{1}{4f^2} \frac{D+F}{2f} \frac{k^{0'} + p_2^{0'}}{E_N(\vec{k}) - p_1^0 - E_N(\vec{k} + \vec{p}_1)} \begin{cases} p_{1z} & m' = +1/2 \\ p_{1x} + ip_{1y} & m' = -1/2 \end{cases} \quad (31)$$

where  $k^{0'}$  and  $p_2^{0'}$  are the energies of  $\vec{k}$  and  $\vec{p}_2$  written in the  $\pi^0\Lambda$  CM frame.

The amplitude corresponding to the diagram of fig. 7(b), is given by

$$-it^{(p\text{-wave})} = -\frac{D+F}{2f} \frac{f_{\Sigma^*\pi\Lambda}}{m_\pi} \frac{f_{K^-p\Sigma^*0}}{m_\pi} \vec{S}^\dagger \cdot \vec{p}_2' \vec{S} \cdot \vec{k}' \vec{\sigma} \cdot \vec{p}_1 \\ \times \frac{1}{M_R - M_{\Sigma^*} + i\Gamma_{\Sigma^*}(M_R)/2} \frac{1}{E_N(\vec{k}) - p_1^0 - E_N(\vec{k} + \vec{p}_1)} \quad (32)$$

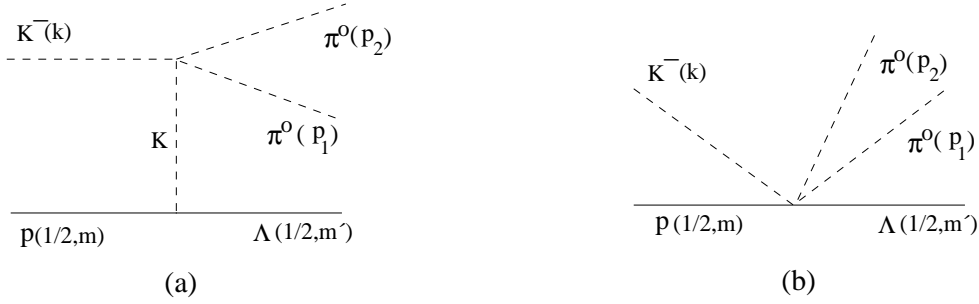


Figure 8: A conventional scheme for  $K^- p \rightarrow \pi^0 \pi^0 \Lambda$

where  $f_{K^- p \Sigma^{*0}}$  is given in [19] by

$$\frac{f_{K^- p \Sigma^{*0}}}{m_\pi} = -\frac{2\sqrt{3} D + F}{5 \cdot 2f}. \quad (33)$$

and

$$\vec{S}^\dagger \cdot \vec{p}'_2 \vec{S} \cdot \vec{k}' \vec{\sigma} \cdot \vec{p}_1 = \begin{cases} -\frac{i}{3} (\vec{p}'_2 \times \vec{k}') \cdot \vec{p}_1 + \frac{2}{3} (\vec{p}'_2 \cdot \vec{k}') p_{1z} + \frac{1}{3} (\vec{p}_1 \cdot \vec{p}'_2) k'_z - \frac{1}{3} (\vec{p}_1 \cdot \vec{k}') p'_{2z} & m' = +1/2 \\ \frac{2}{3} (\vec{p}'_2 \cdot \vec{k}') (p_{1x} + ip_{1y}) + \frac{1}{3} (\vec{p}_1 \cdot \vec{p}'_2) (k'_x + ik'_y) - \frac{1}{3} (\vec{p}_1 \cdot \vec{k}') (p'_{2x} + ip'_{2y}) & m' = -1/2 \end{cases}$$

where the boosted momenta  $\vec{p}'_2$  and  $\vec{k}'$  are obtained as in eq. (29). Next we study the amplitude corresponding to fig. 8. As shown in [22] the contact term of fig. 8(b) just cancels the part of fig. 8(a) which comes from the off shell part of the meson meson amplitude. Hence, using the diagram of fig. 8(a) with the meson meson amplitude calculated on shell accounts for the sum of the two diagrams. We take the  $K^- K^+ \rightarrow \pi^0 \pi^0$  amplitude from [23] and the  $K^- p \Lambda$  vertex from [4] and we obtain

$$-it^{(K^- pole)} = -\frac{1}{4f^2} \left( -\frac{2}{\sqrt{3}} \frac{D+F}{2f} + \frac{1}{\sqrt{3}} \frac{D-F}{2f} \right) \frac{(p_1 + p_2)^2}{(k - p_1 - p_2)^2 - m_K^2} \times \begin{cases} (k - p_{1z} - p_{2z}) & m' = +1/2 \\ -(p_{1x} + p_{2x}) - i(p_{1y} + p_{2y}) & m' = -1/2 \end{cases}. \quad (34)$$

We add all these amplitudes symmetrized to the former ones and recalculate the cross section. Note that the amplitude  $t^{(K^- pole)}$  is already symmetric with respect to the momenta  $p_1$  and  $p_2$  and does not have to be symmetrized again. The results are shown in fig. 9. We find that by themselves the new mechanisms would give a cross section more than one order of magnitude smaller than the experiment, up to 600 MeV/c, indicating that the dominant mechanism by far is the one that we have investigated with the  $\pi \Sigma^*$  tied to the  $\Lambda(1520)$  resonance. Added coherently to the dominant mechanism, these new processes produce a negligible effect around the  $\Lambda(1520)$  peak and they become more visible far away from the resonance where they increase the cross section and help to get a good agreement with the data.

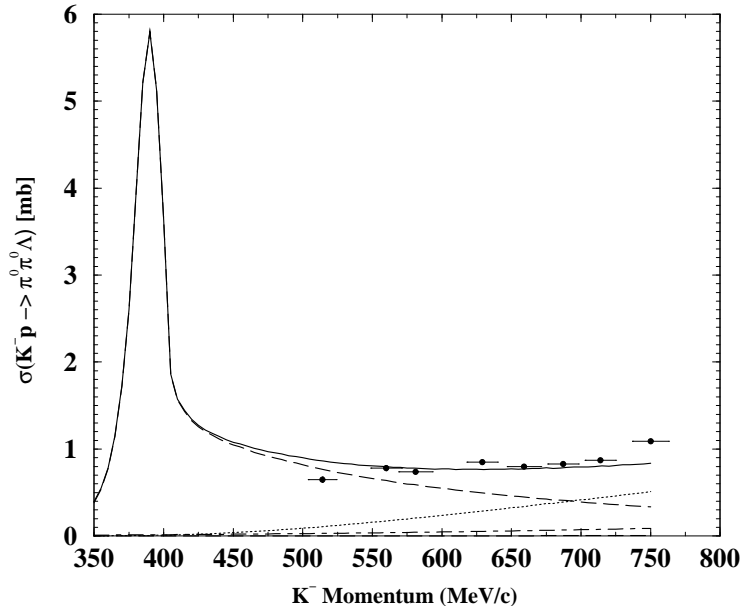


Figure 9: Cross-section as a function of the  $K^-$  momentum. The dot-dashed and dotted lines are the contributions of the diagrams of figs. 7(a) and 7(b) respectively. The dashed line shows the cross section with fig. 5 only and the solid line for a coherent sum of all these diagrams.

Details on the new mechanisms are as follows:

a) The kaon pole term of fig. 8(a) produces a negligible effect in the cross section not visible in fig. 9. The  $K$  propagator reduces the strength of the diagram and the factor  $(p_1 + p_2)^2$  from the  $K^+K^- \rightarrow \pi^0\pi^0$  amplitude also contributes to the small size of the term.

b) The term from the diagram of fig. 7(a) involving the  $s$ -wave  $K^-p \rightarrow \pi^0\Lambda$  amplitude contributes about one fifth of the total cross section at the highest energy of fig. 9 and adds practically incoherently to the  $K^-p \rightarrow \pi^0\Sigma^{*0}$  mechanism.

c) The term from the diagram of fig. 7(b) involving the  $p$ -wave  $K^-p \rightarrow \pi^0\Lambda$  amplitude contributes about one half of the total cross section at the highest energy of fig. 9 and also adds almost incoherently to the other mechanisms.

We also calculate the differential cross section  $d\sigma/dM^2$  as a function of the invariant mass of a pair of  $\pi^0\Lambda$  for two values of  $K^-$  momentum which we plot in fig. 10. We find a good agreement with the experimental curves in [20]. In the figure we can see the  $\Sigma^*(1385)$  peak clearly. We also notice, as in [20], that the effect of symmetrization of the amplitudes with respect to the two final pions is visible in the spectra. Indeed, we see that for  $p_K=659$  MeV/c some strength piles up on the left hand side of the resonance while for  $p_K=750$  MeV/c this strength is moved to higher energies and produces a shoulder on the right hand side. These features are also clear in the experimental data.

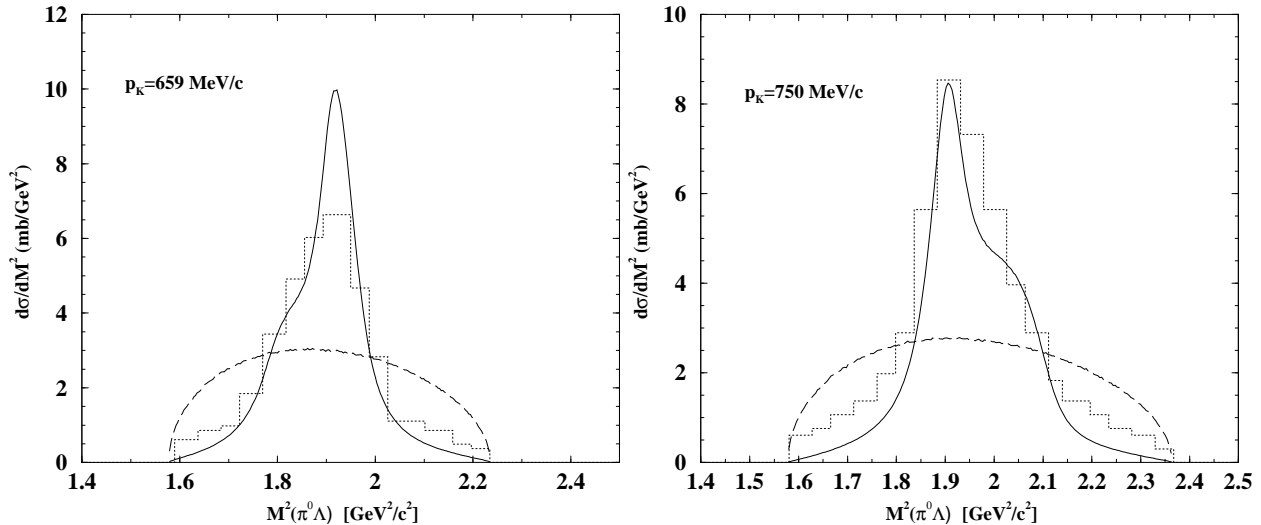


Figure 10:  $d\sigma/dM^2$  as a function of the invariant mass of  $\pi^0\Lambda$  for two values of the  $K^-$  momentum in CM; Left: 659 MeV and Right: 750 MeV. Solid lines represent our results. The dotted histograms are the experimental results from [20] normalized to the total experimental cross section. The dashed lines indicate the phase space normalized to the theoretical cross section.

## 5 Conclusions

We have extended the chiral unitary approach for the interaction of the decuplet of baryons with the octet of mesons, for the case of meson baryon scattering in the region of the  $\Lambda(1520)$  resonance, by including the  $\bar{K}N$  and  $\pi\Sigma$  channels which couple in  $d$ -wave to the main  $s$ -wave channels  $\pi\Sigma^*(1385)$  and  $K\Xi^*(1533)$ . The introduction of these channels allowed us to obtain a more realistic description of the  $\Lambda(1520)$  resonance and make predictions for reactions which evidence the nature of this resonance as a quasibound  $\pi\Sigma^*(1385)$  state. We found a good example in the  $K^-p \rightarrow \pi\Sigma^*(1385)(\pi^0\Lambda)$  reaction which has been measured recently. We found that the strength of the cross section was well reproduced in terms of the large coupling of the  $\Lambda(1520)$  to  $\pi\Sigma^*(1385)$ , which is a prediction of the chiral unitary approach. Both the total cross sections as well as the invariant mass distributions of  $\pi^0\Lambda$  were well reproduced. In addition the theory makes predictions for a large peak of the total cross section of  $K^-p \rightarrow \pi^0\pi^0\Lambda$  for  $K^-p$  energies around the  $\Lambda(1520)$ , and hence below the  $\pi\Sigma^*(1385)$  threshold. The prediction for this cross section is related to the large coupling of the  $\Lambda(1520)$  to  $\pi\Sigma^*(1385)$  in spite of the fact that the  $\pi\Sigma^*(1385)$  is kinematically forbidden. This region falls just below the data measured in the reaction that we analyze. It is then clear that a measurement of the reactions in this region becomes most advisable, and confirmation of the quantitative predictions made here would support the idea of the  $\Lambda(1520)$  as a dynamically generated resonance, and by extension for the other resonances equally generated from the interaction of the decuplet of baryons and octet of mesons.

## Acknowledgments

This work is partly supported by DGICYT contract number BFM2003-00856, and the E.U. EURIDICE network contract no. HPRN-CT-2002-00311. This research is part of the EU Integrated Infrastructure Initiative Hadron Physics Project under contract number RII3-CT-2004-506078.

## References

- [1] S. Eidelman *et al.* [Particle Data Group], Phys. Lett. B **592**, 1 (2004).
- [2] N. Kaiser, P. B. Siegel and W. Weise, Phys. Lett. B **362** (1995) 23
- [3] N. Kaiser, T. Waas and W. Weise, Nucl. Phys. A **612** (1997) 297 [arXiv:hep-ph/9607459].
- [4] E. Oset and A. Ramos, Nucl. Phys. A **635** (1998) 99. [arXiv:nucl-th/9711022].
- [5] J. C. Nacher, A. Parreno, E. Oset, A. Ramos, A. Hosaka and M. Oka, Nucl. Phys. A **678** (2000) 187 [arXiv:nucl-th/9906018].
- [6] J. A. Oller and U.-G. Meißner, Phys. Lett. B **500** (2001) 263. [arXiv:hep-ph/0011146].
- [7] T. Inoue, E. Oset and M. J. Vicente Vacas, Phys. Rev. C **65** (2002) 035204 [arXiv:hep-ph/0110333].
- [8] E. Oset, A. Ramos and C. Bennhold, Phys. Lett. B **527** (2002) 99 [Erratum-ibid. B **530** (2002) 260] [arXiv:nucl-th/0109006].
- [9] C. Garcia-Recio, J. Nieves, E. Ruiz Arriola and M. J. Vicente Vacas, Phys. Rev. D **67** (2003) 076009 [arXiv:hep-ph/0210311].
- [10] D. Jido, J. A. Oller, E. Oset, A. Ramos and U. G. Meissner, Nucl. Phys. A **725** (2003) 181 [arXiv:nucl-th/0303062].
- [11] C. Garcia-Recio, M. F. M. Lutz and J. Nieves, Phys. Lett. B **582** (2004) 49 [arXiv:nucl-th/0305100].
- [12] E. E. Kolomeitsev and M. F. M. Lutz, Phys. Lett. B **585** (2004) 243 [arXiv:nucl-th/0305101].
- [13] S. Sarkar, E. Oset and M. J. Vicente Vacas, Nucl. Phys. A **750** (2005) 294 [arXiv:nucl-th/0407025].
- [14] J. A. Oller, E. Oset and A. Ramos, Prog. Part. Nucl. Phys. **45** (2000) 157 [arXiv:hep-ph/0002193].

- [15] E. Jenkins and A. V. Manohar, Phys. Lett. B **259** (1991) 353.
- [16] J. Gasser and H. Leutwyler, Nucl. Phys. B **250** (1985) 465.
- [17] M. N. Butler, M. J. Savage and R. P. Springer, Nucl. Phys. B **399**, 69 (1993) [arXiv:hep-ph/9211247].
- [18] J. A. Oller and E. Oset, Phys. Rev. D **60** (1999) 074023 [arXiv:hep-ph/9809337].
- [19] E. Oset and A. Ramos, Nucl. Phys. A **679** (2001) 616 [arXiv:nucl-th/0005046].
- [20] S. Prakhov *et al.*, Phys. Rev. C **69** (2004) 042202.
- [21] D. Jido, E. Oset and A. Ramos, Phys. Rev. C **66** (2002) 055203 [arXiv:nucl-th/0208010].
- [22] T. Hyodo, A. Hosaka, E. Oset, A. Ramos and M. J. Vicente Vacas, Phys. Rev. C **68** (2003) 065203 [arXiv:nucl-th/0307005].
- [23] J. A. Oller and E. Oset, Nucl. Phys. A **620** (1997) 438 [Erratum-ibid. A **652** (1999) 407] [arXiv:hep-ph/9702314].

## Appendix

Here we describe in some detail the procedure followed to perform the integration over the three body phase space which was encountered in the evaluation of the cross section for the reaction  $K^- p \rightarrow \pi^0 \pi^0 \Lambda$  due to the various Feynman diagrams described in this work.

For the differential cross section we follow the definition

$$\begin{aligned}
 d\sigma &= (2\pi)^4 \delta^{(4)}(p_1 + p_2 + p_\Lambda - k - p) \frac{2M_N}{v_{rel}} \frac{2M_\Lambda}{2\omega_K} \frac{1}{2E_N} S |Amp|^2 \\
 &\times \frac{d^3\vec{p}_1}{(2\pi)^3 2\omega_1} \frac{d^3\vec{p}_2}{(2\pi)^3 2\omega_2} \frac{d^3\vec{p}_\Lambda}{(2\pi)^3 2E_\Lambda} \quad (A.1)
 \end{aligned}$$

with  $v_{rel} = [(k \cdot p)^2 - m_K^2 M_N^2]^{1/2} / (\omega_K E_N)$  and  $S(= 1/2)$ , the symmetry factor for the two identical  $\pi^0$ . In the  $K^- p$  CM system, the cross section is obtained as

$$\sigma = \frac{M_N M_\Lambda}{\lambda^{1/2}(s, m_K^2, M_N^2)} \int \frac{d^3\vec{p}_1}{(2\pi)^3 2\omega_1} \int \frac{d^3\vec{p}_2}{(2\pi)^3 2\omega_2} \frac{|Amp|^2}{2E_\Lambda} (2\pi) \delta(\sqrt{s} - \omega_1 - \omega_2 - E_\Lambda) \quad (A.2)$$

with  $\vec{p}_\Lambda = -(\vec{p}_1 + \vec{p}_2)$  as a result of the integration over  $\vec{p}_\Lambda$  and using  $2v_{rel}\omega_K E_N = \lambda^{1/2}(s, m_K^2, M_N^2)$ . In order to simplify the angular integration we now make the following coordinate transformation. Assuming  $\phi_1 = 0$  without loss of generality, let us denote by  $\theta_{12}$  the angle between the vectors  $\vec{p}_1$  and  $\vec{p}_2$ . We now generate the vector  $\vec{p}_2$  in a frame in

which the polar angle is  $\theta_{12}$  so that its components with respect to this rotated frame are given by

$$\vec{\tilde{p}}_2 = \begin{cases} p_2 \sin \theta_{12} \cos \tilde{\phi}_2 \\ p_2 \sin \theta_{12} \sin \tilde{\phi}_2 \\ p_2 \cos \theta_{12} \end{cases} \quad (\text{A.3})$$

and the differential is given by  $d^3\vec{\tilde{p}}_2 = -|\vec{\tilde{p}}_2|^2 d|\vec{\tilde{p}}_2| d(\cos \theta_{12}) d\tilde{\phi}_2$ . The  $\delta$  function can now be used to perform the integral over  $\cos \theta_{12}$  and we have

$$\sigma = \frac{M_N M_\Lambda}{\lambda^{1/2}(s, m_K^2, M_N^2)} \frac{1}{8} \frac{1}{(2\pi)^4} \int_{-1}^1 d \cos \theta_1 \int_{m_\pi}^{\omega_{max}} d\omega_1 \int_0^{2\pi} d\tilde{\phi}_2 \int_{m_\pi}^{\omega_{max}} d\omega_2 |Amp|^2 \Theta(1-|A|^2) \quad (\text{A.4})$$

where

$$A = \cos \theta_{12} = \frac{[(\sqrt{s} - \omega_1 - \omega_2)^2 - |\vec{p}_1|^2 - |\vec{p}_2|^2 - M_\Lambda^2]}{2 |\vec{p}_1| |\vec{p}_2|}$$

and

$$\omega_{max} = \frac{s + m_\pi^2 - (m_\pi + M_\Lambda)^2}{2\sqrt{s}}$$

is the maximum energy of the pion which is reached in the case when the other pion and the  $\Lambda$  move together. The original vector  $\vec{p}_2$  is recovered through

$$\vec{p}_2 = R_y(\theta_1) \vec{\tilde{p}}_2 \quad (\text{A.5})$$

where

$$R_y(\theta_1) = \begin{pmatrix} \cos \theta_1 & 0 & \sin \theta_1 \\ 0 & 1 & 0 \\ -\sin \theta_1 & 0 & \cos \theta_1 \end{pmatrix}$$

is the usual rotation matrix for a rotation by an angle  $\theta_1$  around the  $y$ -axis. Note that  $|\vec{p}_2| = |\vec{\tilde{p}}_2|$ .